# Rectangular Scale-Similar Etch Pits in Monocrystalline Diamond

Craig McGray[a*], Richard Allen[a], Marc Cangemi[b], and Jon Geist[a]

[a]Semiconductor Electronics Division, National Institute of Standards and Technology, Gaithersburg, MD 20899
[b] Center for Nanoscale Science and Technology, National Institute of Standards and Technology, Gaithersburg, MD 20899

**Abstract.** Etching of monocrystalline diamond in oxygen and water vapor at 1100 $^{o}$C through small pores in a silicon nitride film produced smooth-walled rectangular cavities. The cavities were imaged by electron microscope and measured by interferometric microscopy. The observed cavities ranged in size from approximately 1 µm up to 72 µm wide, in each case exhibiting smooth, vertical sidewalls, a flat bottom, and a depth equal to half its width. Cavity boundaries were determined to lie along slow-etching (100) crystallographic planes, suggesting the possibility of a powerful class of techniques for high-aspect-ratio bulk micromachining of diamond.

The extreme material properties of diamond make it a compelling material for micro- and nanotechnology applications, including high-power electronics [1], micro-electromechanical systems [2], optical waveguides [3], and solid-state quantum devices [4]. Additionally, the material's hardness, inertness, and resistance to fouling make it an attractive candidate for atomic force microscope (AFM) calibration artifacts and line width standards [5]. Outside of the electronic realm, most diamond devices are at the present time fabricated from polycrystalline

---

* Corresponding author: Fax: 301-975-6021
  E-mail address: craig.mcgray@nist.gov

thin films. However, the material properties of polycrystalline diamond are generally inferior to those of the monocrystalline material and can be much less consistent due to grain structure variations both from batch to batch and through the thickness of an individual film [6].

With recent developments improving the speed and cost of synthesizing monocrystalline diamond substrates, and with achievable substrate dimensions increasing [7-8], the next bottleneck to the development of single-crystal diamond devices may be the difficulty of shaping the material into the necessary features and cavities [9]. Diamond micromachining techniques developed to date use plasma etchants or utilize ion implantation to convert the diamond material to a more volatile $sp^2$-bonded form for removal [9-11]. Ion implantation methods require focused ion beam milling to expose the damaged layers, while plasma etchants create trade-offs between etch rate, mask selectivity, surface roughness, and sidewall angle.

Crystallographic etching techniques have long been used for delineating defects in diamond [12], and orientation-dependent variations in oxidative etch rates have been noted [13,14]. However, oxidative etching of diamond has not yet been explored as a micromachining technique. In contrast, crystallographic etching has been a workhorse technique for micromachining of silicon and other common materials, both in industry and in the research community [15]. A similar technique for diamond could be of considerable value, especially when near-atomically-smooth features are required, as is the case for linewidth standard reference materials [5].

Here we report on deep rectangular etch pits produced by crystallographic etching of monocrystalline diamond in oxygen and water vapor. The etched material was a (100)-oriented intrinsic monocrystalline diamond substrate manufactured by epitaxial chemical vapor deposition. The substrate was cleaned for 15 min by immersion in a 65 $^{\circ}$C solution of sulfuric

acid, peroxymonosulfuric acid, hydrogen peroxide, and water[1]; was rinsed in deionized water; and was blown dry with nitrogen. A coating of 100 nm of stoichiometric silicon nitride was applied by low-pressure chemical vapor deposition performed at 835 $^{\circ}$C in 89 μmol/s of ammonia and 30 μmol/s of dichlorosilane at a pressure of 33 Pa. A novolak-based photoresist film[2] was then spun onto the substrate and cured on a hotplate at 115 $^{\circ}$C. Pinholes in the photoresist layer (due to particles, bubbles, or other non-idealities) were transferred into the silicon nitride by reactive ion etching in $CF_4$ and $O_2$ plasma flows of 19 μmol/s and 3.7 μmol/s, respectively, with 100 W RF power at 8 Pa. Under these conditions, a 5 min etch time was sufficient to penetrate the silicon nitride film to the underlying diamond. The photoresist was then stripped by soaking in an N-methylpyrrolidone-based solvent[3], and the sample was cleaned once again in the sulfuric acid solution, rinsed, and dried, before being transferred to the furnace for etching. The sample was etched for 3 min at atmospheric pressure at a temperature of 1100 $^{\circ}$C in a gas flow mixture of 745 μmol/s oxygen and 1378 μmol/s hydrogen. The hydrogen and oxygen react to yield 1378 μmol/s of water and 56 μmol/s of molecular oxygen.

Upon removal from the furnace, etch pits in the diamond were visible by optical microscopy through the transparent film of silicon nitride. At the center of each etch pit, the pinhole that allowed the etching to occur could be clearly seen, as shown in Figure 1. The silicon nitride film was removed by soaking in a 180 $^{\circ}$C orthophosphoric acid solution[4], and, after rinsing and drying, the substrate was sputter-coated with 10 nm of gold to aid inspection.

Three-dimensional profiles of the etch pits were taken using interferometric microscopy, resulting in the measurements shown in Figure 2. The pits had a square profile in the plane of the substrate and were approximately half as deep as they were wide in each case. Based on this, it

---

[1] Nanostrip, Cyantek Corporation, Fremont, CA
[2] S1813, Microchem Corporation, Newton, MA
[3] Remover PG, Microchem Corporation, Newton, MA
[4] Transetch, Transene Corporation, Danvers, MA

was determined that the etch process was limited by slow-etching {100} planes in each of the three orthogonal axes. Inspection of the sample by electron microscopy confirmed the shape of the cavities, as shown in Figure 3, and revealed additional rectangular etch pits that were too small to be imaged with interferometric microscopy. These pits were observed to have widths as small as 1 μm.

It is hypothesized that the sizes of the etch pits were determined by the flows of reactant and product gasses through the silicon nitride pores, so that larger pores allowed for more rapid etching. Under this hypothesis, the {100} crystal planes remained the slowest-etching planes even as the etch rate ranged from 0.3 μm/min up to 24.0 μm/min. This suggests the possibility of highly anisotropic crystallographic etching protocols whose etch rates could be broadly controlled by adjusting the concentration of reactant gasses.

In summary, this letter contains a description of scale-similar rectangular etch pits formed by oxidation of monocrystalline diamond in molecular oxygen and water vapor. The pits ranged in width from as small as 1 μm up to 72 μm, while maintaining a consistent ratio of width to depth. The results suggest the possibility of controlled crystallographic etching protocols that could be an enabling technique for micromachining single-crystal diamond devices.

## REFERENCES

[1]  Amaratunga GAJ. A dawn for carbon electronics? Science 2002; 297:1657-1658.
[2]  Kohn E, Gluche P, Adamschik M. Diamond MEMS— A new emerging technology. Diamond and Related Materials 1999; 8:934-940.
[3]  Hiscocks MP, Ganesan K, Gibson BC, Huntington ST, Ladouceur F, Prawer S. Diamond waveguides fabricated by reactive ion etching. Optics Express 2008; 16(24): 19512-19519.
[4]  Greentree AD, Fairchild BA, Hossain FM, Prawer S. Diamond integrated quantum photonics. Materials Today 2008; 11(9):22-31.

[5]  Dixson RG, Allen RA, Guthrie WF, Cresswell MW. Traceable calibration of critical-dimension atomic force microscope linewidth measurements with nanometer uncertainty. Journal of Vacuum Science and Technology B 2005; 23(6): 3028-3032.

[6]  Malta DM, von Windheim JA, Wynands HA, Fox BA. Comparison of the electrical properties of simultaneously deposited homoepitaxial and polycrystalline diamond films. Journal of Applied Physics 1995; 77(4): 1536-1545.

[7]  Issaoui R, Achard J, Silva F, Tallaire A, Tardieu A, Gicquel A, Pinault MA, Jomard F. Growth of thick heavily boron-doped diamond single crystals: Effect of microwave power density. Applied Physics Letters 2010; 97: 182101.

[8]  Bogdan G, Nesládek M, D'Haen J, Haenen K, D'Olieslaeger M. Freestanding (100) homoepitaxial CVD diamond. Diamond and Related Materials 2006; 15:508-512.

[9]  Enlund J, Isberg J, Karlsson M, Nikolajeff F, Olsson J, Twitchen DJ. Anisotropic dry etching of boron doped single crystal CVD diamond. Carbon 2005; 43:1839–1842.

[10] Fairchild BA, Olivero P, Rubanov S, Greentree AD, Waldermann F, Taylor RA, Walmsley I, Smith JM, Huntington S, Gibson BC, Jamieson DN, Prawer S. Fabrication of ultrathin single-crystal diamond membranes. Advanced Materials 2008; 20:4793–4798.

[11] Tran DT, Fansler C, Grotjohn TA, Reinhard DK, Asmussen J. Investigation of mask selectivities and diamond etching using microwave plasma-assisted etching. Diamond and Related Materials 2010; 19:778-782.

[12] Malta DP, Posthill JB, Rudder RA, Hudson GC, Markunas RJ. Etch-delineation of defects in diamond by exposure to an oxidizing flame. Journal of Materials Research 1993; 8(6):1217-1219.

[13] de Theije FK, Roy O, van der Laag NJ, van Enckevort WJP. Oxidative etching of diamond. Diamond and Related Materials 2000; 9: 929-934.

[14] de Theije FK, van Veenendaal E, van Enckevort WJP, Vlieg E. Oxidative etching of cleaved synthetic diamond {111} surfaces. Surface Science 2001; 492: 91-105.

[15] Seidel H, Csepregi L, Heuberger A, Baumgärtel H. Anisotropic etching of crystalline silicon in alkaline solutions. Journal of the Electrochemical Society 1990; 137(11): 3612-3626.
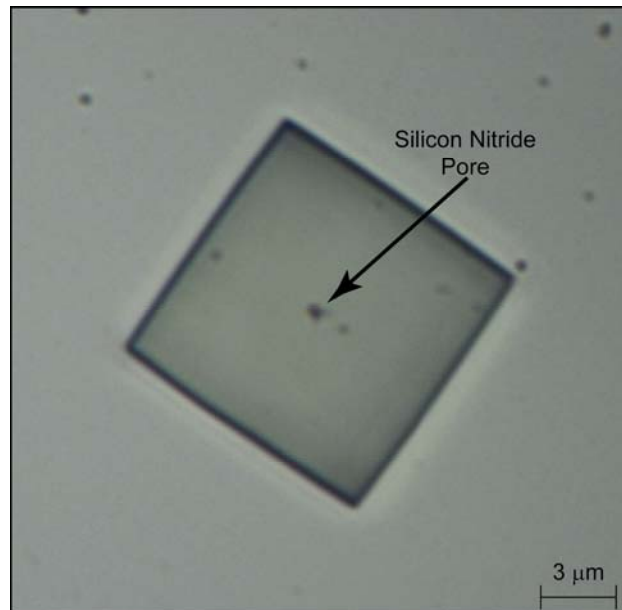
**Figure 1:** An optical micrograph of a rectangular etch pit in (100)-oriented monocrystalline diamond, taken prior to removal of the passivating silicon nitride film. The pore through which the diamond was etched is visible at the center of the pit. The distances between the pore and each of the five bounding faces of the etch pit are approximately equal.
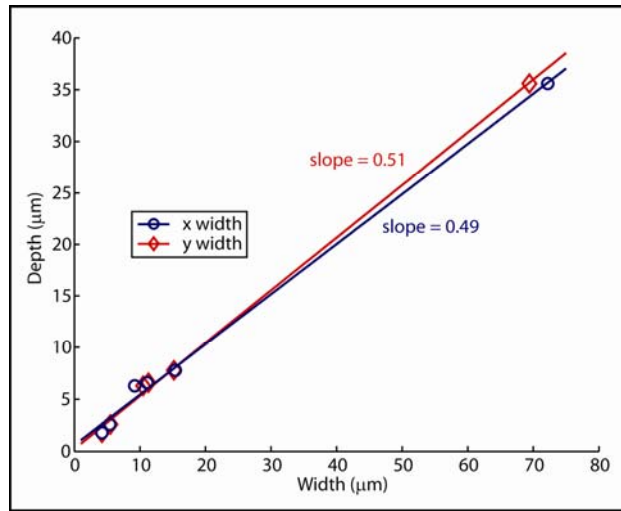
**Figure 2:** Graph of etch pit dimensions, as measured by interferometric microscopy. The ratio of width to depth remains constant across nearly two orders of magnitude.
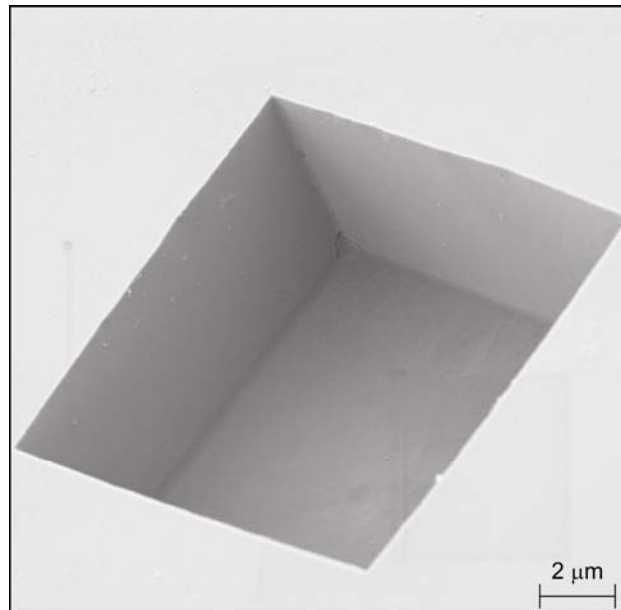


**Figure 3:** Electron micrograph of a rectangular etch pit in monocrystalline diamond, taken at a 45° angle. The pit exhibits smooth, orthogonal sidewalls at {100} orientations, extending 6.2 μm into the diamond bulk.